

# Deep Cooperative Sensing: Cooperative Spectrum Sensing Based on Convolutional Neural Networks

Woongsup Lee, *Member, IEEE*, Minhoe Kim, *Student Member, IEEE*, and  
Dong-Ho Cho, *Senior Member, IEEE*

## Abstract

In this paper, we investigate cooperative spectrum sensing (CSS) in a cognitive radio network (CRN) where multiple secondary users (SUs) cooperate in order to detect a primary user (PU) which possibly occupies multiple bands simultaneously. Deep cooperative sensing (DCS), which constitutes the first CSS framework based on a convolutional neural network (CNN), is proposed. In DCS, instead of the explicit mathematical modeling of CSS which is hard to compute and also hard to use in practice, the strategy for combining the individual sensing results of the SUs is learned with a CNN using training sensing samples. Accordingly, an environment-specific CSS which considers both spectral and spatial correlation of individual sensing outcomes, is found in an adaptive manner regardless of whether the individual sensing results are quantized or not. Through simulation, we show that the performance of CSS can be improved by the proposed DCS with low complexity even when the number of training samples is moderate.

## Index Terms

Cognitive radio network, cooperative spectrum sensing, deep learning, convolutional neural network, correlation.

## I. INTRODUCTION

In cognitive radio networks (CRNs), secondary users (SUs) dynamically utilize the unused channels which are owned by primary user (PU). Given that the top priority of SUs is not to interrupt the operation of the PU, it is of utmost importance to determine whether the PU is

W. Lee is with the Department of Information and Communication Engineering, Gyeongsang National University, Republic of Korea. M. Kim and D.H. Cho are with the School of Electrical Engineering, Korea Advanced Institute of Science and Technology.

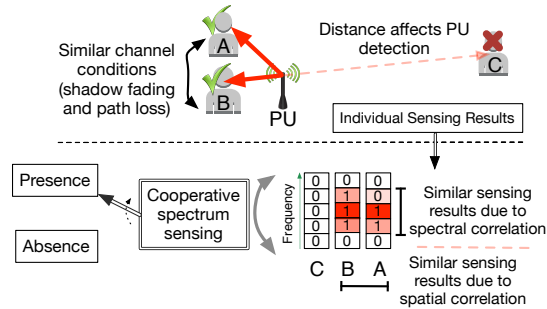


Fig. 1: CSS with correlated individual spectrum sensing.

present or not. Consequently, spectrum sensing to detect the presence of the PU is one of the most important research topic in CRNs [1]–[7].

Given that the sensing results of individual SUs are susceptible to errors due to the fluctuating channel conditions, cooperative spectrum sensing (CSS), where the individual sensing outcomes from multiple SUs are combined to determine the presence of the PU, has been proposed. However, deriving the optimal CSS strategy is complicated due to the correlated channel conditions which depends on the network environment where each SU is situated [2]. For example, SUs which are close to the PU (e.g., SU A and B in Fig. 1) are likely to detect the PU more reliably than SUs which are far away from the PU (e.g., SU C in Fig. 1). Moreover, because of the spatial correlation of wireless channels, SUs which are close to each other (e.g., SU A and B in Fig. 1) are likely to report similar sensing results [5], [6]. In addition, the leakage of transmit power to adjacent bands, i.e., spectral correlation, also needs to be taken into account. The problem becomes more complicated if the SUs and PU can change their positions over time.

For this reason, a simplified system model is widely assumed for CSS which entails a performance degradation. In particular, simple yet efficient CSS strategies such as the  $K$ -out-of- $N$  scheme, which decides that a PU is present if  $K$  SUs out of  $N$  SUs detect the PU, are widely considered in the literature [1], [2], where the individual sensing of SUs is considered to be independent to each other. On the other hand, the authors of [5] and [6] considered the CSS by taking into account the multidimensional correlation in individual sensing results, however, the static SUs without mobility are considered in both works and the proposed scheme requires either the location information of SUs [5] or the distribution of received signal strength (RSS) of each SU [6], which are hard to obtain in practice.

Recently, deep learning has gained considerable attention in many fields of computer science, especially in image processing, speech recognition, and natural language processing, due to the

significant performance gains it can achieve compared with conventional schemes [8]–[10]. A deep neural network (DNN) is a multi-layer network which emulates the neurons of the human brain. In a DNN, the close to optimal strategy to classify data, e.g., speech and images, is learned from a large amount of sample data via the back-propagation algorithm, without the need for developing complicated hand-crafted mathematical models for the data. By building a sufficiently large network, the DNN based model can emulate the behavior of highly nonlinear and complicated systems.

Although DNNs have been mainly applied for image processing and speech recognition so far, they can also be applied in wireless communication systems, especially for classifying communication signals [8], [11]. Given that the surrounding environment, e.g., topology of PU and SUs, can be learned, the DNN based scheme is more adaptive compared with conventional CSS schemes. In [8], the spectrum sensing of a single SU was considered and DNNs were shown to yield a significant performance gain over conventional schemes. Moreover, the authors of [11] showed that the data traffic type can be determined accurately with Long Short Term Memory (LSTM), which is a special type of a recurrent neural network (RNN). In addition, the CSS schemes based on other machine learning techniques except DNN, e.g., support vector machine (SVM), were proposed in [7].

In this paper, we propose deep cooperative sensing (DCS) which is a new DNN-based CSS scheme for CRNs. The contributions of this paper can be summarized as follows.

- 1) We propose DCS, which is a CSS scheme for CRNs employing convolutional neural networks (CNNs), a particular type of DNN. In the proposed scheme, the strategy for combining individual sensing results is learned from training samples, independent of the type of sensing decisions at individual SUs, i.e., both hard decision (HD) and soft decision (SD) sensing are included [3].
- 2) DCS exploits the spatial and spectral correlations of the channels such that the combining strategy for CSS is optimized according to the location of the SUs and the characteristics of the PU in an adaptive manner. To the best of the authors' knowledge, this is the first work that applies deep learning for CSS.
- 3) We evaluate the performance of the proposed scheme based on computer simulations. Our results confirm that the proposed scheme can achieve higher sensing accuracy compared with conventional approaches even when the size of CNN structure is small, i.e., low computational complexity. Moreover, we show that the proposed scheme achieves sufficiently

low sensing errors with small number of training samples, which facilitates the adoption of the proposed scheme in practice.

The remainder of this paper is organized as follows. In Section II, we describe the system model. The proposed DCS scheme is introduced in Section III. Simulation results are provided in Section IV, and Section V concludes the paper.

## II. SYSTEM MODEL AND SPECTRUM SENSING

### A. System Model

We consider the interweave CR system in which SUs opportunistically utilize the idle bands of PU which are found by the CSS [2]. We assume that  $N_{\text{SU}}$  SUs and a single PU are randomly distributed in a given area and move with velocity  $v$  such that the locations of the SUs and the PU change over time, where the locations of SUs are not known to a fusion center which combines the individual sensing results. Moreover, we assume a multi-channel system with  $N_{\text{B}}$  bands whose bandwidth is  $W$ . The PU can simultaneously utilize  $N_{\text{BP}}$  consecutive bands, while the SUs do not know which bands are used by the PU. Furthermore, we assume that the transmit power of the PU in a given band is fixed to  $P$  and can be also leaked to adjacent bands whose proportion of power leakage is  $\eta$ . In addition, we consider the additive white Gaussian noise (AWGN) whose power spectral density is  $N_0$ , where  $w_i^j(m)$  is the noise of SU  $i$  on band  $j$  at time  $m$ .

A simplified path-loss model with path-loss exponent  $\alpha$  and path-loss constant  $\beta$  is adopted for modeling the channel between the PU and the SUs. Let  $d_i(m)$  be the distance between the PU and SU  $i$  at time  $m$ , then the path-loss is  $\beta(d_i(m))^\alpha$ . The effect of multi-path fading,  $g_i^j(m)$ , is also considered where  $i$  is the index of the SU,  $j$  is the index of the band, and  $m$  is the time index. In this work,  $g_i^j(m)$  is modeled as an independent zero-mean circularly symmetric complex Gaussian (CSCG) random variable.

Furthermore, spatially correlated shadow fading is also taken into account [12]. Specifically, we assume that  $h_i(m)$  is the shadow fading of the channel between SU  $i$  and the PU in dB at time  $m$  and it follows a normal distribution with mean zero and variance  $\sigma$  [12]. Then, a normal random variable with zero mean and unit variance, which we denote as  $k_i(m)$  (normalized shadow fading), can be obtained as  $\frac{h_i(m)}{\sigma}$ . Let SU A and SU B be separated by distance  $d_{A-B}$ . Then, the correlation of the normalized shadow fading between these SUs, i.e.,  $k_A(m)$  and  $k_B(m)$ , which we denote as  $\rho_{\text{cor}}(d_{A-B})$ , is modeled as [5], [6], [12]

$$\rho_{\text{cor}}(d_{\text{A-B}}) = \mathbb{E} [k_{\text{A}}(m)k_{\text{B}}(m)] = e^{\left(-\frac{d_{\text{A-B}}}{d_{\text{ref}}}\right)}, \quad (1)$$

where  $d_{\text{ref}}$  denotes a reference distance whose value depends on the environment, e.g., rural or urban. Accordingly, the shadow fading of two SUs which are nearby will have a high correlation, i.e., the SUs experience similar shadow fading. In our system model, the RSS of the PU at two SUs which are close to each other will be similar due to both path-loss and shadow fading, which results in similar sensing outcomes.

### B. Spectrum Sensing

We assume that the SUs perform individual spectrum sensing which is based on the energy detection in all  $N_{\text{B}}$  bands for a time period of  $\Delta t$  where  $N_{\text{ED}}$  channel samples are collected for each sensing attempt. Moreover, we assume that SUs do not transmit data during CSS, e.g., quiet period in the IEEE 802.22 [2], such that the individual sensing is not affected by the interference from the transmission of other SUs.

Regarding the state of the PU, two hypotheses, which are  $\mathcal{H}_0$  and  $\mathcal{H}_1$ , are considered, where  $\mathcal{H}_0$  represents the case where the PU is absence while  $\mathcal{H}_1$  represents the case where the PU is presence. Then, the received signal of SU  $i$  on band  $j$  at time  $m$ , which we denote as  $y_i^j(m)$ , can be written as

$$y_i^j(m) = \begin{cases} \kappa_i(m)g_i^j(m)x(m) + w_i^j(m), & \text{for } \mathcal{H}_1 \text{ and } j \in B_P \\ \sqrt{\eta}\kappa_i(m)g_i^j(m)x(m) + w_i^j(m), & \text{for } \mathcal{H}_1 \text{ and } j \in B_A \\ w_i^j(m), & \text{otherwise} \end{cases} \quad (2)$$

where  $\kappa_i(m) = \sqrt{\frac{P}{\beta(d_i(m))^{\alpha} 10^{\frac{h_i(m)}{10}}}}$  and  $x(m)$  is the data transmitted by PU at time  $m$  where  $|x(m)| = 1$ . Moreover,  $B_P$ ,  $B_A$ , and  $B_V$  are the set of bands which are occupied by the PU, which are affected by the leaked power of PU and which are not affected by the PU, respectively.

Given that the energy detection is considered, the signal strength of channel has to be accumulated. Let  $T_i^j$  be the accumulated RSS of SU  $i$  on band  $j$ . Then  $T_i^j$  can be written as follows.

$$T_i^j = \frac{1}{N_{\text{ED}}} \sum_{m=1}^{N_{\text{ED}}} |y_i^j(m)|^2. \quad (3)$$

It should be noted that  $N_B \times N_{\text{SU}}$  individual sensing outcomes are collected by the CRN. We let  $\mathbf{T}$  be the matrix of the accumulated RSS of all SUs.

After calculating  $T_i^j$ , SU  $i$  can report either the measured RSS for each band (SD), i.e.,  $T_i^j$ , or binary sensing results for each band using a sensing threshold  $\gamma$  (HD), which we denote as  $\hat{T}_i^j$ . In the latter case, the SU reports 1 if  $\gamma \leq T_i^j$  and reports 0 otherwise. Obviously, the signaling overhead is much larger for the SD compared with HD, however, a higher sensing accuracy can be achieved with SD.

Based on the individual sensing results, the fusion center of CRN determines the presence of the PU by combining the individual sensing outcomes. The accuracy of spectrum sensing can be denoted by the probability of false alarm ( $P_{\text{FA}}$ ) which is the probability that an SU falsely detects a PU when no PU is present and the probability of miss detection ( $P_{\text{MD}}$ ) which is the probability that an SU fails to detect a PU when one is present [2].

When SD is used, the optimal fusion rule can be obtained by comparing two conditional probabilities which are  $f_{\mathbf{T}}(T_1^1, T_1^2 \cdots T_{N_{\text{SU}}}^{N_B} | \mathcal{H}_0)$  and  $f_{\mathbf{T}}(T_1^1, T_1^2 \cdots T_{N_{\text{SU}}}^{N_B} | \mathcal{H}_1)$ , where  $f_{\mathbf{T}}(T_1^1, T_1^2 \cdots T_{N_{\text{SU}}}^{N_B} | \cdot)$  is the joint conditional probability density function (PDF) of entire sensing results. Although  $f_{\mathbf{T}}(T_1^1, T_1^2 \cdots T_{N_{\text{SU}}}^{N_B} | \mathcal{H}_0)$  can be summarized as  $f(T_1^1 | \mathcal{H}_0) f(T_1^2 | \mathcal{H}_0) \cdots f(T_{N_{\text{SU}}}^{N_B} | \mathcal{H}_0)$  which is easy to calculate, where  $f(\cdot | \mathcal{H}_0)$  is the conditional PDF of individual sensing result when a PU is absence,  $f_{\mathbf{T}}(T_1^1, T_1^2 \cdots T_{N_{\text{SU}}}^{N_B} | \mathcal{H}_1)$  is hard to calculate due to spatially and spectrally correlated wireless channel. Moreover, in order to calculate  $f_{\mathbf{T}}(T_1^1, T_1^2 \cdots T_{N_{\text{SU}}}^{N_B} | \mathcal{H}_1)$ , the distance between SUs, and the distance between SUs and PU have to be known, which are hard to obtain in the practical system. The use of optimal fusion rule becomes more challenging as SUs and the PU change their positions due to the mobility.

On the other hand, when HD is used, each SU will report  $\hat{T}_i^j$  which is either 0 or 1 according to the value of  $T_i^j$ . Given that the values of  $\hat{T}_i^j$  are not independent to each other, i.e.,  $\mathbb{E}(\hat{T}_{i_1}^{j_1} \hat{T}_{i_2}^{j_2}) \neq \mathbb{E}(\hat{T}_{i_1}^{j_1}) \mathbb{E}(\hat{T}_{i_2}^{j_2})$ , all possible outcomes of  $\hat{T}_i^j$ , whose cardinality is  $2^{N_B \times N_{\text{SU}}}$ , have to be examined to derive the optimal decision policy and this requires huge computational overhead, especially when the number of SUs is large. The problem can be simplified by assuming that  $\hat{T}_i^j$  is independent and identically-distributed (i.i.d.) such that the number of SUs which report 0 and 1 is sufficient to derive the final CSS decision<sup>1</sup>. However, in practice, the effects of the spectral and spatial

<sup>1</sup>In this case, the number of SUs which report  $\hat{T}_i^j = 1$  when the PU is absence ( $\mathcal{H}_0$ ) and those report  $\hat{T}_i^j = 0$  when the PU is presence ( $\mathcal{H}_1$ ) can be modeled as the Binomial random variable whose success probabilities are  $\Pr(\hat{T}_i^j = 1 | \mathcal{H}_0)$  and  $\Pr(\hat{T}_i^j = 0 | \mathcal{H}_1)$ , respectively, and appropriate decision criteria can be found consequently [1].

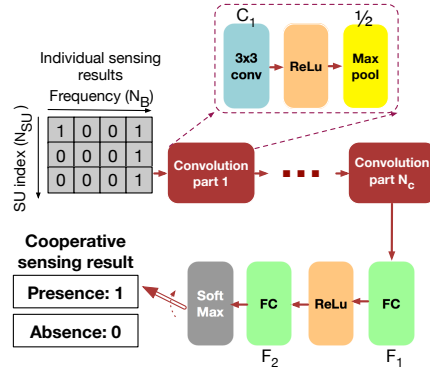


Fig. 2: CNN model for deep cooperative sensing.

correlation of wireless channel on individual sensing outcomes have to be taken into account in order to achieve higher sensing accuracy. Therefore, from the discussions above, we can conclude that the derivation and utilization of mathematically optimal CSS is hard in practice and new yet efficient approach which considers correlations of wireless channel has to be devised.

### III. DEEP COOPERATIVE SENSING

In DCS, the CNN model is used to combine individual sensing results to determine the presence of the PU. CNNs have been widely used in deep learning research to classify images by exploiting their spatial characteristics. In CNN, multi-dimensional convolution is applied to an image to extract its spatial features. The recent success of CNNs in visual classification [9], [10] motivates the adoption of CNNs for CSS, because similar to the correlation of nearby pixels in images, the individual sensing outcomes from nearby SUs and adjacent bands are likely similar due to their spatial and spectral correlation, i.e.,  $\mathbb{E}[(T_i^j - \mathbb{E}[T_i^j])(T_{i+e_1}^{j+e_2} - \mathbb{E}[T_{i+e_1}^{j+e_2}])] > 0$  for  $e_1, e_2 = -1, 0, +1$ . In the following, we first describe the structure of the DCS and then discuss how DCS can be trained to detect the presence of the PU.

#### A. Structure of DCS

The proposed CNN structure for DCS is composed of two parts, which are the convolution part at the front of the network and the fully connected (FC) part at the back of the network, as shown in Fig. 2. First, in our proposed scheme, individual sensing results from different bands and SUs constitute the two dimensional input data for the CNN which is fed into the convolution part, unlike the DNN based spectrum sensing considered in [8] where the in-phase and quadrature-phase of the temporal signal are used to define a two dimensional matrix. The elements of input matrix can be either binary for HD or continuous for SD.

In our CNN structure,  $N_C$  convolution parts which are composed  $3 \times 3$  convolution layer ( $3 \times 3$  conv.), rectifier linear unit (ReLU) layer, and max pooling layer, are connected in tandem. The convolution layer performs spatial convolution of the input data such that the spatial features of the input data can be extracted. The size of each spatial filter in the convolution layer is set to  $3 \times 3$  because as can be concluded from [10], the  $3 \times 3$  convolution is sufficient to extract the spatial features of the input data. Accordingly, let  $X_{\text{conv}}$ ,  $W_{\text{conv}}$ , and  $Y_{\text{conv}}$  be the input, weights, and output of the convolution layer. Then,  $Y_{\text{conv}}[m, n] = \sum_{\epsilon_1=0}^2 \sum_{\epsilon_2=0}^2 X_{\text{conv}}[\epsilon_1+m-1, \epsilon_2+n-1] W_{\text{conv}}[\epsilon_1, \epsilon_2]$ . The depth of the convolution layer for  $i$ -th convolution part is set to  $C_i$  which can be adjusted according to the size of input data, e.g.,  $C_i$  has to be large<sup>2</sup> when  $N_{\text{SU}}$  and  $N_{\text{B}}$  is large. The stride, which is the step size used in the convolution filter, is set to 1 and zero padding is used, so that the size of the output remains the same as that of the input.

After the spatial features have been extracted, the ReLU layer introduces non-linearity to the CNN [10]. When the input of the ReLU layer is  $X_{\text{ReLU}}$ , the output is given by  $\max(X_{\text{ReLU}}, 0)$ , such that negative inputs are blocked. Without the ReLU, the CNN model would be linear and unable to classify non-linear behavior. The ReLU layer is followed by the max pooling layer which reduces the size of the data. With the max pooling layer, the computational overhead can be efficiently reduced without significant performance loss as shown in [9].

The FC part performs classification based on the output of the convolution part by gathering the results of feature extraction. To this end, the FC layer mixes all the data from the convolution part using the multiplication of the weights and the addition of biases. Specifically, the output of  $m$ -th FC layer,  $Y_{\text{FC}}^m$ , becomes  $Y_{\text{FC}}^m = W_{\text{FC}}^m X_{\text{FC}}^m + b_{\text{FC}}^m$ , where  $X_{\text{FC}}^m$ ,  $W_{\text{FC}}^m$  and  $b_{\text{FC}}^m$  are the inputs, weights and biases for the  $m$ -th FC layer, respectively. In DCS, we consider two FC layers whose depth (number of hidden node) are  $F_1$  and  $F_2$ , respectively. Moreover, an additional ReLU layer is placed between two FC layers in order to introduce non-linearity. Then the output of the FC layers is fed into the softmax operator in which the final decision on whether the PU is present or not is made using the softmax function. Let index 0 and 1 denote the absence and the presence of the PU, respectively, and  $X_S$  be the input of the softmax operation. Then, in our model, the CRN determines that the channel is idle if  $\frac{e^{W_S^0 X_S}}{\sum_{i=0}^1 e^{W_S^i X_S}} > \frac{e^{W_S^1 X_S}}{\sum_{i=0}^1 e^{W_S^i X_S}}$ , and otherwise it concludes that the channel is occupied by the PU, where  $W_S^i$  is a weight matrix of the softmax operator.

<sup>2</sup>However, through simulations, we show that a relatively small  $C_i$ , i.e., small sized CNN structure, compared with what is normally used for image classification [9], [10], can achieve sufficiently high sensing accuracy, because unlike image classification where typically hundreds of different classes have to be distinguished, in our system model, we only need to classify two classes, namely the presence and absence of the PU.



### B. Training of PRNet

In order to train the proposed DCS, individual sensing outcomes are collected first. Then, the proposed DCS is trained, i.e., the weights and biases of each layer are found, to minimize the cross entropy loss,  $\mathcal{L}$ , using off-the-shelf stochastic gradient descent algorithms, i.e., adaptive moment estimation. Specifically, the cross entropy loss can be written as  $\mathcal{L} = -\sum_{\epsilon=0}^1 l_{\epsilon} \log(Y_S^{\epsilon})$  where  $Y_S^{\epsilon}$  is the output of softmax operator, i.e.,  $Y_S^{\epsilon} = \frac{e^{W_S^{\epsilon} X_S}}{\sum_{i=0}^1 e^{W_S^i X_S}}$ , and  $l_{\epsilon}$  is the target label whose value is either 0 or 1. When the PU is presence,  $l_0 = 0$  and  $l_1 = 1$ , and if the PU is absence,  $l_0 = 1$  and  $l_1 = 0$ . Note that the cross entropy loss is minimized when the estimated value matches with the correct label, i.e.  $Y_S^{\epsilon} = 1$  for  $l_{\epsilon} = 1$ , such that the DCS can be trained to accurately detect the presence of the PU.

In our proposed scheme, the multiple CNN models with different permutations of SU index are trained simultaneously and the trained model whose accuracy is highest, is chosen. Through the permutation, we can find the proper order of SU index such that the sensing results of neighboring SUs can be placed nearby in the input data, which improves the performance of DCS. It is worth noting that the optimal permutation of SU index cannot be known in advance because the location information of SUs is unavailable. Although we do not show in the performance evaluation, we have observed that the sensing error can be decreased by 17% through the permutation of SU index.

Thereafter, the trained model can be used to determine the presence of PU based on the individual sensing results. Although the training of DCS might require huge overhead, the inference of final sensing result can be conducted with relatively low overhead as shown later in the performance evaluation such that the real-time operation of our proposed scheme is feasible.

## IV. PERFORMANCE EVALUATION

In this section, the performance of the proposed DCS is examined. Our performance evaluation is implemented using Tensorflow which is an open-source software library for machine intelligence developed by Google. We assume that a single PU and multiple SUs which move at  $v = 3$  km/h, are randomly deployed in a  $200 \text{ m} \times 200 \text{ m}$  area. Moreover, the number of bands is set to 16 where  $W = 10$  MHz and  $N_{\text{Bp}}$  is randomly chosen from 1 to 3, i.e., the PU can utilize upto three bands simultaneously. Furthermore, we assume that  $\eta = -20$  dB,  $P = 23$  dBm,  $\beta = 10^{3.453}$ ,  $\alpha = 3.8$ ,  $\sigma = 7.9$  dB, and  $d_{\text{ref}} = 50$  m [12], [13]. Moreover, we assume that  $N_C = 3$ ,  $C_1 = C_2 = C_3 = F_1 = F_2 = 8$ . Note that we have used a relatively small number

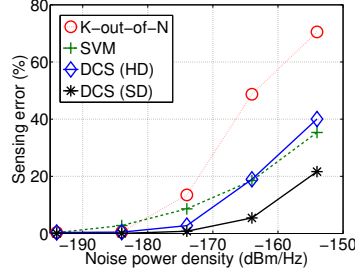


Fig. 3: Noise power density vs. sensing error when  $N_{\text{SU}} = 32$  and  $N_{\text{sample}} = 200$ .

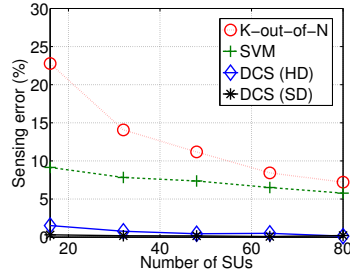


Fig. 4: Number of SUs vs. sensing error when  $N_0 = -174$  dBm/Hz and  $N_{\text{sample}} = 200$ .

of weights and biases<sup>3</sup> for CNN structure such that the training and inference of DCS can be performed with low complexity.

We assume that each SU performs individual spectrum sensing every 2 seconds, i.e.,  $\Delta t = 2$  seconds [2]. Threshold  $\gamma$  is set to  $-107$  dBm [2] such that when HD is used, each SU sends 1 if the RSS exceeds  $\gamma$  and sends 0 otherwise. When SD is used, each SU reports the measured RSS, i.e.,  $T_i^j$ . For performance evaluation,  $N_{\text{sample}}$  samples are used to train the model and the 2000 samples are used for the evaluation where these data sets are generated by computer simulation<sup>4</sup>.

For the performance metric, we consider the sensing error which is the sum of the probability of false alarm ( $P_{\text{FA}}$ ) and the probability of miss detection ( $P_{\text{MD}}$ ) [5]. We examine the sensing error of our proposed scheme for both SD and HD. Moreover, conventional CSS based on the  $K$ -out-of- $N$  scheme is considered where the value of  $K$  is selected such that  $(P_{\text{FA}} + P_{\text{MD}})$  is minimized. Furthermore, conventional CSS based on SVM with the linear kernel is also considered which shows the lowest sensing error in [7].

<sup>3</sup>When the number of SUs is 32, the number of weights in our CNN model is 2264, which is smaller than that for image classification (61,000,000) [9].

<sup>4</sup>In this work, a synthetic data set is used for learning, whereas in a practical system, real data would be used. Nevertheless, the performance evaluation based on the synthetic data can also provide meaningful insights regarding the performance of the proposed scheme [8].

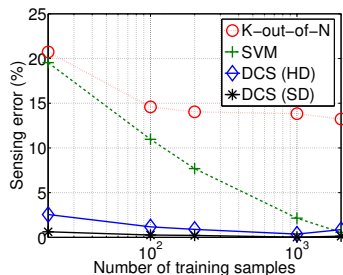


Fig. 5: Number of training samples vs. sensing error when  $N_{\text{SU}} = 32$  and  $N_0 = -174$  dBm/Hz.

In Fig. 3, we show the sensing error vs. the noise density for  $N_{\text{SU}} = 32$  and  $N_{\text{sample}} = 200$ . We observe that the sensing error increases as the noise density increases due to the inaccurate individual sensing results. Moreover, we can also find that the sensing error of DCS is lower than those of conventional schemes, i.e.,  $K$ -out-of- $N$  scheme and SVM scheme, when  $N_0 \leq -164$  dBm/Hz, and the DCS with SD shows the lowest sensing error in all cases, which highlights the benefits of the proposed scheme. Especially, we can find that the DCS with SD shows sufficiently low sensing error, i.e., sensing error is less than 21% even when the power of the noise is very large, e.g.,  $N_0 = -154$  dBm/Hz. The DCS with HD shows worse sensing accuracy than that with SD because individual sensing results contain less information [3].

In Fig. 4, we examine the sensing error as function of the number of SUs for  $N_0 = -174$  dBm/Hz and  $N_{\text{sample}} = 200$ . As can be observed from Fig. 4, the performance of CSS is improved as the number of cooperating SUs increases, which coincides with our intuition. We can also confirm that DCS significantly outperforms conventional schemes, especially when the number of SUs is small.

The sensing error by varying the number of training samples for  $N_{\text{SU}} = 32$  and  $N_0 = -174$  dBm/Hz is shown in Fig. 5. Given that the decision policy of  $K$ -out-of- $N$  scheme and SVM scheme is also determined based on training samples, the sensing error of those schemes also changes as  $N_{\text{sample}}$  changes. We can again confirm that DCS achieves lower sensing error compared with conventional schemes. It is worth noting that DCS shows sufficiently low sensing error even when the number of training samples is small, i.e.,  $N_{\text{sample}} = 100$ , such that the overhead of data collection for training data will be small.

Finally, in Fig. 6, we evaluate the computation time of considered CSS schemes as function of the number of SUs for  $N_0 = -174$  dBm/Hz and  $N_{\text{sample}} = 200$ . Although the computation time of DCS is larger than those of conventional schemes, it is reasonably small, e.g., the computation

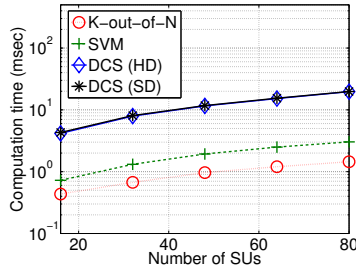


Fig. 6: Number of SUs vs. computation time when  $N_0 = -174$  dBm/Hz and  $N_{\text{sample}} = 200$ .

time of DCS is less than 20 msec in all cases, such that our proposed scheme can be operated in real-time manner.

## V. CONCLUSIONS

In this paper, a novel CNN-based CSS scheme for CRN was proposed, which is the first attempt to use deep learning for CSS. In DCS, the strategy for combining the binary or real valued individual sensing results of the SUs is learned using CNN. Through simulations we investigated the performance of the proposed scheme and found that DCS outperforms conventional CSS schemes. We also found that DCS can detect the PU accurately with small sized CNN structure, even when the number of training samples is small, which verifies the applicability of our proposed scheme in practice.

## REFERENCES

- [1] E. Peh, Y.-C. Liang, Y. L. Guan, and Y. Zeng, "Optimization of cooperative sensing in cognitive radio networks: A sensing-throughput tradeoff view," *IEEE Trans. Veh. Technol.*, vol. 58, no. 9, pp. 5294–5299, Nov. 2009.
- [2] W. Lee and D.-H. Cho, "Enhanced spectrum sensing scheme in cognitive radio systems with MIMO antennae," *IEEE Trans. Veh. Technol.*, vol. 60, no. 3, pp. 1072–1085, Mar. 2011.
- [3] J. So and W. Sung, "Group-based multibit cooperative spectrum sensing for cognitive radio networks," *IEEE Trans. Veh. Technol.*, vol. 65, no. 12, pp. 10 193–10 198, Dec. 2016.
- [4] H. Reyes, S. Subramaniam, N. Kaabouch, and W. C. Hu, "A spectrum sensing technique based on autocorrelation and Euclidean distance and its comparison with energy detection for cognitive radio networks," *Computers & Electrical Engineering*, vol. 52, pp. 319 – 327, May 2016.
- [5] D. Xue, E. Ekici, and M. C. Vuran, "Cooperative spectrum sensing in cognitive radio networks using multidimensional correlations," *IEEE Trans. Wireless Commun.*, vol. 13, no. 4, pp. 1832–1843, Apr. 2014.
- [6] A. W. Min and K. G. Shin, "An optimal sensing framework based on spatial RSS-profile in cognitive radio networks," in *Proc. of IEEE SECON*, Rome, Italy, Jun. 2009.
- [7] K. M. Thilina, K. W. Choi, N. Saquib, and E. Hossain, "Machine learning techniques for cooperative spectrum sensing in cognitive radio networks," *IEEE J. Sel. Areas Commun.*, vol. 31, no. 11, pp. 2209–2221, Nov. 2013.

- [8] T. J. O’Shea, J. Corgan, and T. C. Clancy, “Convolutional radio modulation recognition networks,” in *Proc. of EANN*, Aberdeen, U.K., Sep. 2016.
- [9] A. Krizhevsky, I. Sutskever, and G. E. Hinton, “Imagenet classification with deep convolutional neural networks,” in *Proc. of NIPS*, Stateline, NV, Dec. 2012, pp. 1097–1105.
- [10] K. Simonyan and A. Zisserman, “Very deep convolutional networks for large-scale image recognition,” *arXiv preprint arXiv:1409.1556*, 2014.
- [11] T. J. O’Shea, S. Hitefield, and J. Corgan, “End-to-end radio traffic sequence recognition with deep recurrent neural networks,” *arXiv preprint arXiv:1610.00564*, 2016.
- [12] A. Algans, K. Pedersen, and P. Mogensen, “Experimental analysis of the joint statistical properties of azimuth spread, delay spread, and shadow fading,” *IEEE J. Sel. Areas Commun.*, vol. 20, no. 3, pp. 523–531, Apr. 2002.
- [13] IEEE 802.20, “IEEE 802.20 channel models document,” January 2007.